Catalysis Today 187 (2012) 88–96

Contents lists available at SciVerse ScienceDirect

Catalysis Today

journal homepage: www.elsevier.com/locate/cattod

Al-pillared montmorillonite as a support for catalysts based on ruthenium sulfide in HDS reactions

A. Romero-Pérez[a], A. Infantes-Molina[b], A. Jiménez-López[a], E. Roca Jalil[c], K. Sapag[c], E. Rodríguez-Castellón[a,*]

[a] Dpto. de Química Inorgánica, Cristalografía y Mineralogía (Unidad Asociada al ICP-CSIC), Facultad de Ciencias, Universidad de Málaga, Campus de Teatinos, 29071 Málaga, Spain
[b] Instituto de Catálisis y Petroleoquímica, CSIC, c/Marie Curie, 2, Cantoblanco, 28049 Madrid, Spain
[c] Laboratorio de Sólidos Porosos, Instituto de Física Aplicada (INFAP), CONICET – Universidad Nacional de San Luís, Argentina

ARTICLE INFO

Article history:
Received 14 June 2011
Received in revised form
22 November 2011
Accepted 12 December 2011
Available online 14 January 2012

Keywords:
Al pillared montmorillonite
Hydrodesulfurization, Ruthenium sulfide
Dibenzothiophene

ABSTRACT

Sulfided ruthenium supported catalysts based on an Al pillared montmorillonite, with different Al contents, have been prepared and characterized by XRD, S_{BET}, TEM, XPS, and tested in the hydrodesulfurization (HDS) of dibenzothiophene (DBT). The role of the Al content in the catalytic activity of RuS_2 based catalysts was studied. The activity and selectivity of the catalysts studied in the HDS of DBT suggest that Al pillared montmorillonite could be of interest as a low cost support for this reaction.

1. Introduction

The presence of sulfur in fossil fuels is one of the most important causes of environmental pollution. The burning of diesel in combustion engines releases sulfur into the environment as SO_x, and when it combines with atmospheric water, it becomes what is known as 'acid rain' [1]. As a consequence, irreversible ecological harm is done to the biodiversity of the planet, contributing to the degradation of our environment. The main process in the petrochemical industry for the removal of sulfur from crude oil is the hydrotreating process, which is carried out with Co(Ni)MoS sulfided catalysts [2,3] as active phases and γ-alumina as a support. To date, these catalysts have been used due to the excellent activity shown. Notwithstanding, the increasing demand of diesel oil, the lower quality of the remaining petroleum reserves and the tighter environmental restrictions with regards to sulfur content in diesel fuel has led to the search for highly efficient catalytic phases which can almost completely remove any sulfur containing molecules. In the last few decades, a plethora of articles has been devoted to the hydrotreating activity of Co(Ni)MoS based catalysts using different supports, promoters or synthetic approaches in order to improve the activity and stability of the hydrodesulfurization (HDS) catalysts, although the active phase has hardly been modified [4,5]. The incorporation of small quantities (0.3–0.8 wt.%) of noble metals (Rh, Ru, Pd and Pt) to a Mo/Al_2O_3 system produced an enhancement [6] of the catalytic activity due to synergic effects. Unsupported transition metal sulfides were plotted into a curve called the "volcano plot" where the HDS activity per mole of metal versus the M—S bond strength was plotted, the most active being the RuS_2 phase [7].

Several unsupported transition metal sulfides (TMS) have been synthesized and tested in the HDS reaction of DBT [8]. In general, TMS catalysts are stable under the severe conditions employed in the hydrotreating process, this fact being of utmost importance [9]. Among all the TMS studied, RuS_2 was the most active catalyst. Raje et al. [10] studied the removal of individual sulfur compounds of a coal-derived naphtha with several bulk TMS. They found that ruthenium and rhodium were the most active with total sulfur removal levels being greater than 90%. Moreover, in a simultaneous removal of sulfur, nitrogen and oxygen compounds from a coal-derived naphtha, RuS_2 displayed the highest activity for all three of the hydrotreating processes [11]. When supported, its catalytic activity and stability depend strongly on the preparation method. Owing to this there are various points to consider during its preparation since according to the literature [12,13] RuS_2 must have a pyrite-type structure, called laurite, which should be highly dispersed in the support. To this end, experimental variables such as the precursor salt employed, the sulfiding gas mixture, the sulfiding temperature and the catalyst support employed influence the catalytic activity of the prepared materials [12,13]. In this sense, it is

* Corresponding author. Tel.: +34 952131873; fax: +34 952132000.
E-mail address: castellon@uma.es (E. Rodríguez-Castellón).

0920-5861/$ – see front matter © 2011 Elsevier B.V. All rights reserved.
doi:10.1016/j.cattod.2011.12.020

suggested that calcination be avoided after impregnation, and that $RuCl_3$ be used as a precursor salt and a sulfiding mixture be used in the absence of hydrogen in order to avoid the formation of metallic ruthenium. The latter is very difficult to sulfide [12,14] and requires a higher sulfidation temperature in order to form highly stable RuS_2 particles with a pyrite-type structure presenting a better exposure of the crystallographic planes (111) and (210), on which the reaction takes place [15,16]. In reference to this, De los Reyes et al. [13] pointed out that the faces formed at a low sulfiding temperature are more active for biphenyl (BP) hydrogenation (HYD) while those formed at higher temperatures are more active for thiophene HDS [13]. Considering the influence of the support employed, the most widely used is alumina [12,13,17], although SBA-15 [18] and MCM-41-type mesoporous materials [19] and MgF_2 [14] have been used with improved performances, mainly due to the mesoporous texture of SBA-15 and MCM-41.

In recent years, pillared clays (PILC) [20] have been studied as adsorbents, supports and acid catalysts not only for their performance but also due to their low cost [21,22]. One of the most important applications for these materials has been as a catalyst support for the selective catalytic reduction (SCR) of NO by NH_3 [23–25]. Pillared clays have also been used as a support for NiMo catalysts for HDS and HDN reactions [26], where both the impregnation method and the order of incorporation of the metals (Ni and Mo) influenced the dispersion of the active phases. To date, information about ruthenium sulfide catalysts supported on alumina-pillared clays has been scarce in the literature. However, an aluminum-pillared bentonite was used as a ruthenium catalyst support for the 1-butene hydrogenation reaction [27] and Pérez-Zurita et al. [28] used a commercial montmorillonite clay as a support for RuS_2 catalysts. The formation of the aluminum pillars and the introduction of the metal into the interlayer space were done simultaneously. The results obtained indicated that after the pillaring process, an increase in the surface area of the pillared clays, as well as a good dispersion of ruthenium, were observed. They tested the RuS_2 catalysts in a thiophene HDS reaction and their results showed conversions of between 3 and 21% at 280 °C.

In this work, supported RuS_2 catalysts on aluminum-pillared clays, with different aluminum contents were synthesized in order to study the role of the clay in the formation and activity of the RuS_2 phase in the DBT HDS reaction and the influence of the aluminum content on the catalytic activity.

2. Experimental

2.1. Materials

The support used in this study was an aluminum-pillared clay, prepared by pillaring a natural montmorillonite (from the Alto Valle region, Argentina), used as received, with Al^{3+} ions. The formula of the parent montmorillonite is $Si_4Al_{1.36}Mg_{0.27}Fe_{0.25}O_{10}(OH)_2Na_{0.53}$, where the cation exchange capacity is 0.89 mequiv./g of clay. Ruthenium(III) chloride, $RuCl_3{\cdot}nH_2O$ (~41 wt.% Ru, from Fluka) was used as the ruthenium precursor salt. The chemical products used in the reactivity study were dibenzothiophene (Aldrich 98%) in *cis*-, *trans*-decahydronaphthalene (Sigma–Aldrich 98%). The gases employed were H_2S/N_2 10/90 (v/v) (Air Liquide 99.99%), He (Air Liquide 99.99%), H_2 (Air Liquide 99.999%) and N_2 (Air Liquide 99.9999%).

2.2. Preparation of catalysts

Four aluminum-pillared clays with different mequiv. $Al^{3+}\ g^{-1}$ dried clay ratios were used as supports for the RuS_2 catalysts. The synthesis of the aluminum-pillared clay was carried out from a pillaring agent, which was prepared from the hydrolysis of an $AlCl_3{\cdot}6H_2O$ 0.2 M solution with NaOH 0.5 M (OH^-/Al^{3+} molar ratio of 2). NaOH was added dropwise to the aluminum chloride solution at 60 °C under vigorous stirring. The mixture was then stirred overnight at room temperature to obtain the pillaring agent. The solution used for pillaring contains Al_{13} Keggin polycations (the precursor of the pillars) that can be ion exchanged with the charge compensating cations of the montmorillonite clay. A montmorillonite suspension of 3% (w/v) was prepared and stirred for an hour. The pillaring agent was then added dropwise while stirring at room temperature. The mixture obtained was stirred for approximately 1 h and left to settle for 12 h to allow the solid to be deposited at the bottom. The solid was recovered and flushed in order to remove residual salts. Washing was carried out with distilled-water dialysis membranes until the conductivity was that of the distilled water. Finally the solid was dried at 60 °C overnight and calcined at 500 °C for 1 h at a heating rate of 10 °C min^{-1}, thus obtaining the aluminum-pillared clay. The mequiv. $Al^{3+}\ g^{-1}$ dried clay ratios employed to synthesized the aluminum-pillared clays were of 5, 10, 15 and 20 and the obtained solids denoted as PILC Al 5, PILC Al 10, PILC Al 15, and PILC Al 20, respectively. The Si/Al ratio of the parent montmorillonite is 2.67, while that for pillared-clays ranges between 2.29 and 1.97.

The incorporation of ruthenium into the aluminum-pillared clay was carried out by the incipient wetness impregnation method. First an aqueous solution of ruthenium(III) chloride ($RuCl_3.nH_2O$), with the corresponding amount of ruthenium, was added to the pelletized support (0.85–1 mm). All the catalysts prepared here had a constant ruthenium loading of 7 wt.% (0.000745 mol $g_{support}{}^{-1}$). Once the supports were impregnated, they were air-dried, giving the catalyst precursors denoted as *prec Al x*, where *x* is the mequiv. $Al^{3+}\ g^{-1}$ clay (x = 5, 10, 15 and 20). Finally, they were sulfided in situ at atmospheric pressure with a H_2S/N_2 (10/90, v/v) flow of 60 mL min^{-1} and heated from room temperature (rt.) to the sulfidation temperature (Ts) (2 h) at a heating rate of 10 °C min^{-1} to obtain the sulfided catalysts. The catalysts will be referred as Al 5, Al 10, Al 15 and Al 20, accordingly.

2.3. Characterization techniques

X-ray diffraction patterns (XRD) of the precursor, sulfided and spent catalysts were obtained with an X'Pert PRO MPD Philips diffractometer (PANanalytical), using monochromatic CuKα radiation (λ = 1.5406 Å). The $K\alpha_1$ radiation was selected with a Ge (1 1 1) primary monochromator. The X-ray tube was set at 45 kV and 40 mA.

Transmission electron micrographs of the precursor and sulfided catalysts were obtained using a Philips CM 200 Supertwin-DX4 microscope. Samples were dispersed in ethanol and a drop of the suspension was put on a Cu grid (300 mesh).

The textural properties (S_{BET}, V_p, d_p) of the sulfided catalysts were obtained from the N_2 adsorption-desorption isotherms at −196 °C measured with a Micromeritics ASAP 2020 apparatus. Prior to the measurements, samples were outgassed overnight at 200 °C and 10^{-2} Pa. Surface areas were determined using the Brunauer–Emmett–Teller equation and a nitrogen molecule cross section of 16.2 $Å^2$. The pore size distribution was calculated by applying the NLDFT method. The total pore volume was calculated from the adsorption isotherm at $P/P_0 = 0.95$, according to the Gurvich rule. The microporous volume was calculated using the α-plot method.

X-ray photoelectron spectra of the sulfided and spent catalysts were collected using a Physical Electronics PHI 5700 spectrometer with non-monochromatic Al Kα radiation (300 W, 15 kV, and 1486.6 eV) with a multi-channel detector. Spectra of pelletized samples were recorded in the constant pass energy mode at 29.35 eV, using a 720 μm diameter analysis area. Charge

referencing was measured against adventitious carbon (C 1s at 284.8 eV). A PHI ACCESS ESCA-V6.0 F software package was used for acquisition and data analysis. A Shirley-type background was subtracted from the signals. Recorded spectra were always fitted using Gaussian–Lorentzian curves in order to determine the binding energies of the different element core levels more accurately.

2.4. Catalytic activity measurements

For the catalytic test, the HDS of DBT was chosen, which was performed in a high-pressure fixed-bed continuous-flow stainless steel catalytic reactor (9.1 mm in diameter, and 230 mm in length), operated in the down-flow mode. The reaction temperature was measured with an interior placed thermocouple in direct contact with the catalyst bed. The organic feed was prepared by dissolving the proper amount of DBT (10,000 ppm) in *cis*-, *trans*-decalin. Each solution was supplied by means of a Gilson 307SC piston pump (model 10SC). For the activity tests, 0.5 g of catalyst was used (particle size 0.85–1.00 mm) and was diluted with silicon carbide (0.85 mm) to 3 cm^3. Prior to the activity test, the catalyst precursors were sulfided at atmospheric pressure with a H_2S/N_2 (10/90, v/v) flow of 60 mL min^{-1} by heating from rt. to 500 °C (2 h) with a heating rate of 10 °C min^{-1}. The sulfiding mixture in absence of hydrogen avoids the formation of metallic ruthenium which is more difficult to sulfide. Catalytic activities were measured at different temperatures (260–360 °C), under 3.0 MPa of H_2, with a flow rate of 100 mL min^{-1} and with hourly space velocities (WHSV) of 32 h^{-1}. The evolution of the reaction was monitored by collecting liquid samples after 60 min at the desired reaction temperature. These liquid samples were kept in sealed vials and subsequently analyzed by gas chromatography (Shimadzu GC-14B, equipped with a flame ionization detector and a capillary column, TBR-14, coupled to an automatic Shimadzu AOC-20i injector).

For these catalysts, the main products of the HDS reaction were biphenyl (BP), cyclohexylbenzene (CHB), bicyclohexyl (BCH), benzene (B) and cyclohexane (CH). The total conversion of the HDS reaction was calculated from the ratio of converted DBT/initial DBT. The selectivity to the different reaction products was calculated considering BP, CHB, B and CH as the only products obtained from HDS. Assuming that the reaction is pseudo-first order, then the reaction rate constants of HDS (k_{HDS}) were calculated according to Eq. (1):

$$k_{HDS} = -\left(\frac{F}{W}\right)\ln(1-x) \quad (1)$$

in which, F is the feed rate of dibenzothiophene (mol min^{-1}), W is the catalyst mass (g) and x is the fractional conversion.

3. Results and discussion

3.1. Catalytic activity in the HDS of DBT

RuS_2 based catalysts supported on aluminum-pillared clays were tested in the dibenzothiophene (DBT) hydrodesulfurization (HDS) reaction at different temperatures (260–360 °C), under 3.0 MPa of H_2, with a flow rate of 100 mL min^{-1} and with hourly space velocities (WHSV) of 32 h^{-1}. Fig. 1 depicts the evolution of the conversion for all the catalysts.

As can be clearly seen from this figure, the catalytic activity strongly depends on the support used. The support acidity determined by NH_3-TPD measurements, through out acidity values ranging from 330 to 360 μmol NH_3 g^{-1} for all the pillared clays, ruling out the support acidity as an important factor to understand the activity of the ruthenium sulfide phase. At low reaction temperatures, all the catalysts present similar conversion values, but differences arise when the reaction temperature is increased.

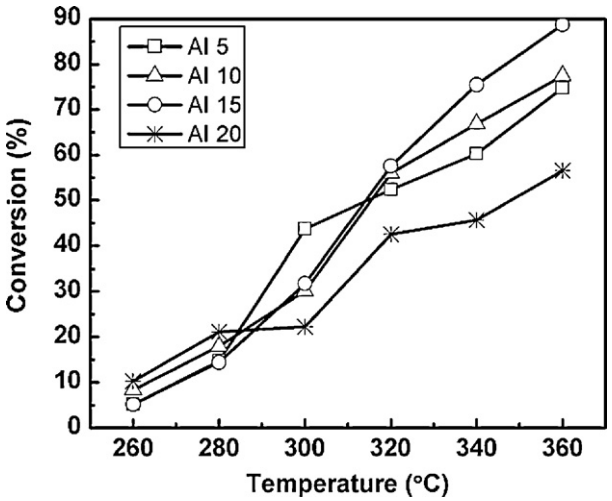

Fig. 1. HDS conversion of RuS_2 based catalysts supported on aluminum-pillared clays as a function of the reaction temperature.

There is a compensatory effect, the isokinetic temperature was calculated as described by Exner [29] by plotting log k versus T^{-1}, and the found value was 292 °C. At temperatures higher than 292 °C clear different catalytic behaviors were observed. The Al 15 catalyst reaches the highest DBT conversion value at 360 °C (90%), followed by Al 10 (77%) and Al 5 (74%). These data suggest that the higher the aluminum content, the better the results, with the exception of Al 20, that exhibits a lower conversion value (57%).

The increasing activity with temperature can be attributed to the creation of either coordinatively unsaturated sites (CUS) or vacancies around the metal; such sites are formed by metal sulfide reduction in a large excess of hydrogen. A CUS site has the function of electron-withdrawing, interacting with electrodonating organic molecules such as the DBT molecule [30–32].

The stability of the catalysts was studied by following the reaction for 12 h on stream at 360 °C. The evolution of the conversion with the reaction time is plotted in Fig. 2. From this figure several conclusions can be drawn: the Al 15 and Al 10 catalysts that gave the highest initial activities, suffer a slight deactivation with time on stream, the conversion decreasing from 85% to 60% for the Al 15 catalyst and from 73% to 56% for the Al 10 one; Al 20 gives the lowest conversion values but without any deactivation detected during the test; and the catalyst with the lowest aluminum

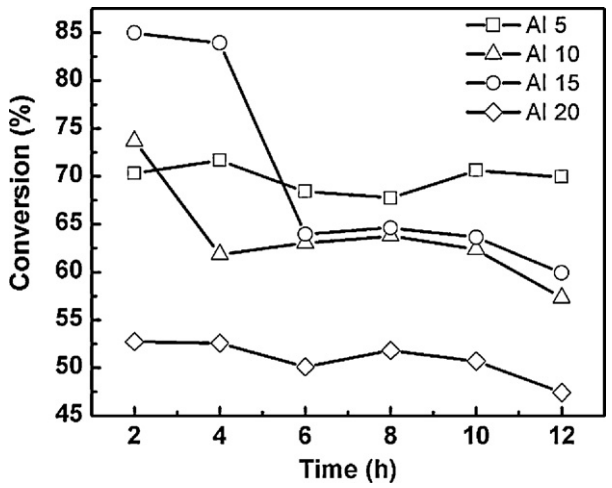

Fig. 2. Evolution of the conversion at 360 °C, as a function of the reaction time.

Table 1
Rate constants for the sulfided catalysts in the DBT HDS reaction.

Catalyst	Reaction temperature (°C)						Stability test at 360 °C (12 h)
	260	280	300	320	340	360	
	$k \times 10^5$ (mol gcat^{-1} min^{-1})						
Al 5	0.15	0.46	1.68	2.16	2.69	4.02	3.6
Al 10	0.25	0.58	1.05	2.39	3.22	4.35	2.4
Al 15	0.15	0.45	1.12	2.51	4.10	6.36	2.6
Al 20	0.32	0.69	0.73	1.61	1.78	2.43	1.9

content, Al 5, proved to be the most active and stable catalyst, with constant conversion of 70%.

From conversion values and by applying Eq. (1), the rate constants at all reaction temperatures and after the stability tests were calculated, and the corresponding values are shown in Table 1. The k_{HDS} increases with the temperature, presenting Al 15 catalyst the highest catalytic activity at 360 °C. However, when this catalyst is maintained at 360 °C for 12 h its activity decays, decreasing the k_{HDS} a 60%; followed by Al 10 with a loss of activity of 45%; while Al 5 and Al 20 catalysts hardly change their initial activity at 360 °C, i.e., they both are the most stable ones.

With regards to the selectivity values, the literature fully describes the dibenzothiophene HDS reaction taking place along two different pathways [33]. The first one, called the direct desulfurization route (DDS), gives biphenyl (BP) as the main product; and the second one, called the hydrogenation (HYD) pathway, gives cyclohexylbenzene (CHB) and bicyclohexyl (BCH) as the main products. Here, in all cases, the products detected were BP, CHB, BCH with cyclohexane (CH) and benzene (B) in minor quantities, coming from the cracking of the former. The BP/CHB ratio is determined by the pathways followed. In our case this ratio was in all cases close to 7 at 360 °C, indicating the DDS route as dominant for these catalytic systems with high temperatures. However, at lower reaction temperatures (<320 °C) the reaction products BCH (bicyclohexil), B (benzene), and CH (cyclohexane) were also observed.

The evolution of the selectivity for the ruthenium sulfide based catalysts as a function of reaction temperature is depicted in Fig. 3. In all cases, and as previously pointed, the product coming from the DDS route, BP, is the main reaction product whose formation increases with temperature. The CHB production goes down as expected, because the hydrogenation is not favored at high temperatures. However, the selectivity presented by Al 20 is slightly different (Fig. 3D), since it is the only catalyst that produces BCH at low temperatures (10–20%) up to 300 °C. From 260 to 300 °C the selectivity to BCH decreases and that of CH increases, suggesting the cracking of BCH molecule as responsible for CH formation over Al 20 catalyst.

3.2. Characterization results

3.2.1. XRD

The X-ray diffraction technique allows us to identify the different crystalline phases present. In order to know if the RuS_2 phase has been formed, the X-ray diffraction profiles of both fresh and spent catalysts after temperature testing were recorded and are shown in Fig. 4.

The alumina pillared supports present similar d_{001} values (18.0–18.5 Å), typical of this type of materials. The diffractograms of freshly sulfided catalysts (Fig. 4a) show several diffraction peaks. In all cases, the diffraction lines located at 2θ = 4.8, 19.8, 35.1 and 61.9° are due to the aluminum-pillared clay pure support; while those found at 2θ values of 27.5°, 31.8, 45.7 and 54.1°, belong to the [1 1 1], [2 1 0], [2 1 1], and [3 1 1] crystallographic planes of the RuS_2 phase with a pyrite-type structure (PDF Card No. 00-012-0737). Comparing the diffractograms, it can be seen that the Al 15 catalyst has the least well defined and least intense RuS_2 diffraction peaks, indicating a lower and less crystalline active phase formation, i.e., a better dispersion. Thus, considering the main diffraction line of RuS_2 phase located at 2θ = 31.8°, and by applying the Scherrer equation, the particle size was calculated. The particle size follows the order: Al 20 (10.9 nm) > Al 5 (7.5 nm) > Al 10 (6.9 nm) > Al 15 (5.9 nm).

In order to know the effect of the reduction conditions employed in the HDS reaction on the RuS_2 phase stability, the X-ray diffraction patterns of spent catalysts were also recorded (Fig. 4b). The diffractograms of spent catalysts show a considerable decrease in the intensity of the diffraction lines from the RuS_2 phase, indicating that a loss of the diffraction domains occurs during the catalytic test, probably due to the partial reduction of ruthenium sulfide into metallic ruthenium as previously reported [17,18]. Catalyst Al 10 suffers the greatest decrease in the RuS_2 diffraction signal intensity and catalyst Al 15 has a broad shoulder at ca. 2θ = 43° corresponding to the [1 0 1] plane of the metallic phase, indicating the formation of this phase during the catalytic test. Catalyst Al 10 does not have such a shoulder leading us to conclude that a partial reduction of the RuS_2 phase occurs but to a lesser extent than that observed in the case of Al 15. The formation of metallic ruthenium cannot be ruled out in the other catalysts, since particles with a dimension smaller than the detection limit of XRD could have been formed.

3.2.2. N_2 adsorption-desorption at −196 °C

The textural properties of the supports and catalysts were obtained by N_2 adsorption-desorption isotherms at −196 °C. The shape of the adsorption-desorption isotherms (not shown here) were classified, according to IUPAC, as a combination of I type isotherm at low relative pressures and IIb type isotherm at higher relative pressures, with an hysteresis loop H4 type [34]. Such isotherms are characteristic of slit-shaped pores or assemblies of platy particles. The calculated specific surface area, micropore volume and total pore volume of the supports and sulfided catalysts are compiled in Table 2. After the pillaring process, the clays suffer

Table 2
Textural properties of the supports and sulfided catalysts.

	S_{BET} (m^2/g)	V_T[a] (cm^3/g)	$V_{\mu p}$[b] (cm^3/g)
Supports			
Natural montomorillonite	64	0.11	0.01
PILC AL 5	184	0.15	0.06
PILC AL 10	279	0.18	0.10
PILC AL 15	283	0.19	0.11
PILC AL 20	285	0.17	0.10
Sulfided catalysts			
Al 5	118	0.09	0.03
Al 10	148	0.16	0.04
Al 15	179	0.12	0.06
Al 20	149	0.10	0.05

[a] V_T Pore total volumen.
[b] $V_{\mu p}$ Microporous volumen.

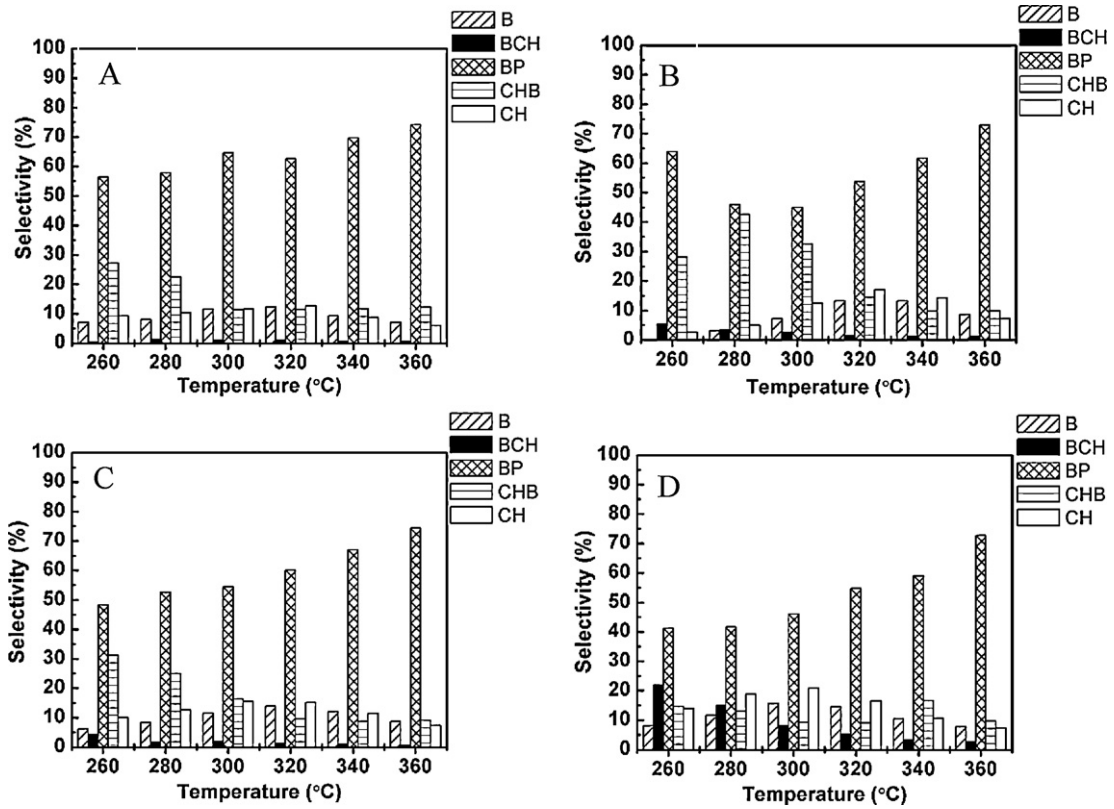

Fig. 3. Selectivity of (A) Al 5; (B) Al 10; (C) Al 15; (D) Al 20 catalysts, where B, BCH, BP, CHB and CH stand for benzene, bicyclohexyl, biphenyl, cyclohexylbenzene and cyclohexane, respectively.

an important increase in the surface area with regards to the parent montmorillonite. The pillared clays present very similar values with the exception of PILC AL 5 with the lowest surface area. Considering the Si/Al ratio obtained from the chemical composition of the pillared clays, the sample PILC Al 5 has the highest value and the change in the ratio for the other samples is not very important and suggests that the addition of higher amounts of Al^{3+} ions has no new effects and therefore the textural properties of the clays hardly change.

After the incorporation of the precursor salt and subsequent sulfidation, the specific surface area of the sulfided catalysts is lower than that of the pristine supports. This is attributed to the location of the active phase at the entrance of the porous structure, causing a partial blockage of the interlayer space of the aluminum-pillared clay. From the data compiled in Table 2, it can be seen that the micropore volume undergoes a considerable decrease after metal incorporation, confirming the previous statement. Catalyst Al 5 suffers a smaller decrease in surface area with regards to its pristine support, although the textural properties of this support are the lowest of the catalysts studied. The pore size distribution, calculated by the NLDFT method [35] ranged in all cases between 11 and 12 Å and those of the pure supports ranged from 14 to 16 Å.

3.2.3. TEM

Transmission electron microscopy was performed in order to elucidate the size, morphology and distribution of the active phase. Fig. 5 shows the micrographs of both sulfided and spent catalysts. In all cases the lamellar structure of aluminum-pillared clays are clearly observed.

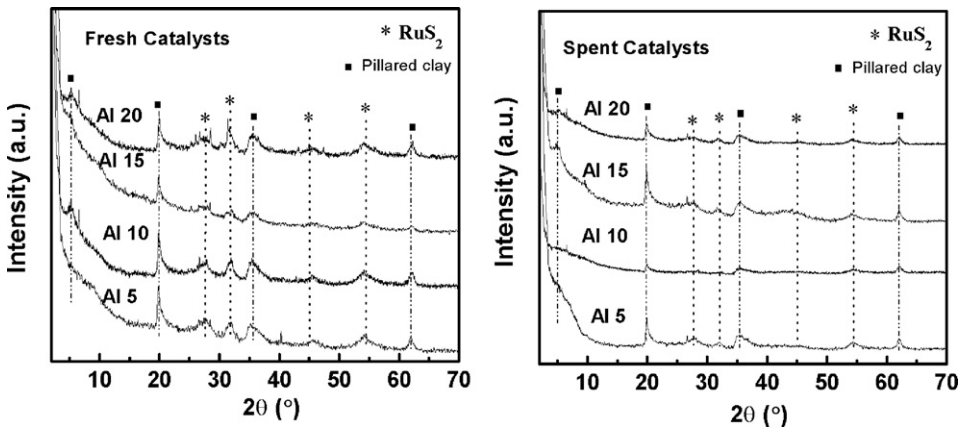

Fig. 4. X-ray diffraction profiles of fresh and spent catalysts after temperature test.

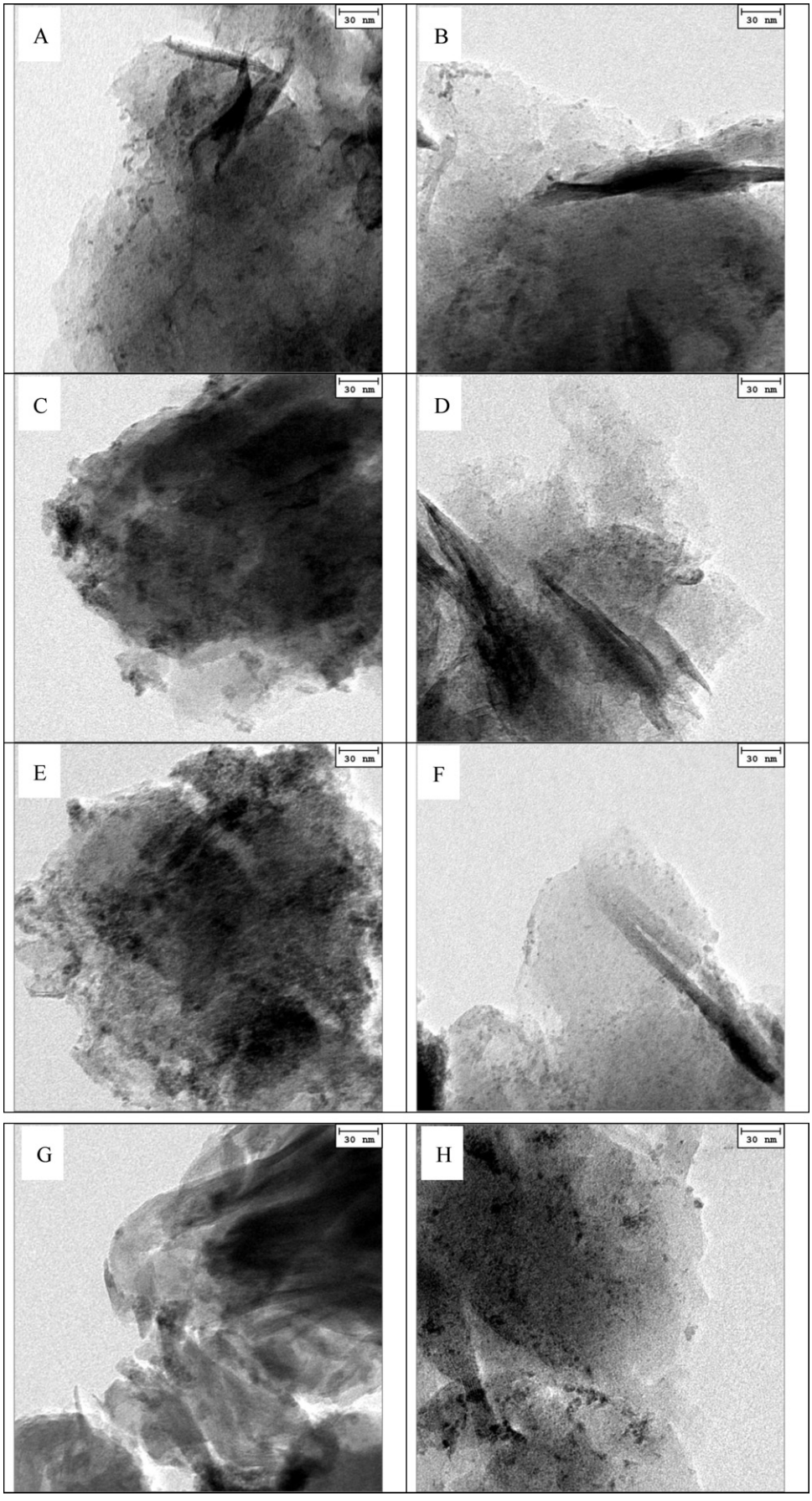

Fig. 5. TEM micrographs of fresh (A) Al 5; (C) Al 10; (E) Al 15; (G) Al 20 and spent catalysts (B) Al 5; (D) Al 10; (F) Al 15; (H) Al 20.

Table 3
Spectral parameters of fresh and spent catalysts.

Sample	Binding Energy (eV)			Atomic ratio	
	Ru $3p_{3/2}$		S $2p_{3/2}$	Ru/(Al + Si)	S/Ru
	RuS_2	Ru^{n+}	S_2^{2-}		
Fresh catalyst					
Al 5	461.5 (91.8)	463.1 (8.2)	162.6	0.12	2.9
Al 10	461.8 (85.9)	465.5 (14.1)	162.8	0.04	2.8
Al 15	461.6 (85.8)	463.9 (14.2)	162.8	0.14	2.5
Al 20	461.6 (89.8)	464.4 (10.2)	162.4	0.06	2.3
Spent catalyst					
Al 5	461.8 (90.8)	464.8 (9.2)	162.6	0.15	1.8
Al 10	461.8 (84.1)	465.1 (15.9)	162.7	0.07	1.3
Al 15	462.1 (83.7)	464.6 (16.3)	162.9	0.12	1.1
Al 20	461.6 (89.8)	464.1 (10.2)	162.5	0.20	2.1

In brackets the percentage of each species on the support surface.

The general trend observed is the presence of highly dispersed RuS_2 particles and some agglomerates which are bigger than the interlayer space. Particles lower than 10 nm are observed in all cases that are located outside the pores as long as the pore size is 11–12 Å, in all cases. Moreover, the micrographs show a probable restructuring of the active phase for catalysts Al 10 and Al 15, where a change of the active phase morphology is noticeable after the catalytic reaction (Fig. 4D and F). This is also apparent for catalyst Al 20 but this sample is less affected than the others. Meanwhile, the Al 5 sample was the least affected morphologically and hence its catalytic activity has probably hardly been affected.

3.2.4. XPS

The chemical state of the elements present on the catalyst surface was studied by XPS. To this end O 1s, Si 2p, Al 2p, Ru 3p, S 2p and Cl 2p signals were analyzed for sulfided and spent catalysts. The O 1s, Al 2p, and Si 2p BE values were 538.2 eV, 75.4 eV and 103.4 eV, respectively. These values remained practically constant in all cases and also after the catalytic test, demonstrating the high stability of the Al pillared clay during the reaction. The Cl 2p signal was not detected in any case, which indicates that chloride species are removed during the sulfidation process. The Ru $3p_{3/2}$, S $2p_{3/2}$ binding energy values, as well as the Ru/(Si + Al) and S/Ru atomic ratios of sulfided and spent catalysts, are shown in Table 3.

The Ru 3p core level spectra of sulfided catalysts (Fig. 6A) can be decomposed into two contributions. The first ranges between 461.5 and 462.1 eV, and is ascribed to a RuS_2 compound [36]; the second ranges between 463.1 and 465.5 eV, being attributed to Ru^{n+} species [37–39]. The S 2p signal was studied to establish whether S_2^{2-} ions were formed after the sulfiding procedure. The S 2p spectrum (Fig. 6B) gives an asymmetrical signal fitted into one doublet, S $2p_{3/2}$ and S $2p_{1/2}$ coming from the spin–orbit splitting. The BE value of the S $2p_{3/2}$ component ranges between 162.4 and 162.9 eV, and is assigned to S_2^{2-} forming a pyrite-type structure [12,13,40] such as RuS_2.

The influence of the clay used as a support on the Ru 3p and S 2p core level spectra reveals that catalyst Al 5 gives the most intense Ru 3p and S 2p signals, indicating a surface enrichment of such compounds on the catalyst surface. Contrary to this, catalyst Al 10 gives the weakest intensities of these signals due to a greater dispersion of the active phase on this catalyst after sulfidation. Meanwhile, catalysts Al 15 and Al 20 show a similar ruthenium and sulfur distribution. The analysis of the Ru 3p and S 2p core level spectra for spent catalysts are shown in Fig. 6B and D. It can be seen that BE (Table 3) slightly changed after the catalytic test. The main differences found are the increase in the intensity of the Ru $3p_{3/2}$ band assigned to Ru^{n+} species (~463.5 eV) and the correspondent increase of the percentages of such species on the catalyst surface for Al 10 and Al 15 catalysts, along with a decrease in the S 2p signal intensity for the Al 15 catalyst. This indicates a loss of sulfur during the test, as previously found from the XRD results. In fact, by considering the S/Ru atomic ratio values, which are higher than the theoretical one (2.0) for the fresh catalysts, and the decrease in these values after the catalytic test, we can confirm the loss of sulfur during the catalytic test. This is a much more important consideration for catalysts Al 10 and Al 15 (1.3 and 1.1), which could explain the loss of activity found for these systems during the stability test. On the other hand, the most stable catalysts (Al 5 and Al 20) have a S/Ru atomic ratio close to 2 after the catalytic test, indicating that the pyrite structure on these two catalysts is more stable.

3.3. Discussion

The hydrodesulfurization of DBT over ruthenium sulfide supported on Al pillared clays mainly involves the direct desulfurization route (DDS) with biphenyl being the main product found in all cases. Hence the hydrogenolysis reaction is dominant over the hydrogenation reaction. All RuS_2 catalysts are active in the DBT HDS reaction. Nonetheless, Al 10 and Al 15 suffer a considerable decrease in their catalytic activity after 6 h on stream, while Al 5 and Al 20 catalysts were found to be the most stable, with Al 5 giving a constant conversion of ca. 70% after 12 h on stream. These catalytic results are of the up most importance when considering the search for a support which avoids a difficult synthetic procedure.

Characterization results from XRD and XPS reveal that the formation of RuS_2 with a pyrite-type structure occurs after the sulfidation process. From XRD patterns it can be inferred that the least stable catalysts are those that suffer a greater sulfur loss during the catalytic test, diminishing the intensity of RuS_2 diffraction lines or even showing diffraction signals arising from the presence of metallic ruthenium, as in the case of Al 15. This is also confirmed by XPS, where the partial reduction of the RuS_2 phase during the catalytic test is clearly observed as shown by the S/Ru atomic ratios found for the spent catalysts, explaining the loss of activity exhibited in catalysts Al 10 and Al 15. Moreover, micrographs of the spent catalysts (Fig. 4D and F) show a possible change in the morphology of the active phase which could be related to the decrease in catalytic activity of catalysts Al 10 and Al 15. This result is a consequence of using high temperatures and strong reducing conditions, i.e. severe reaction conditions which could lead to a restructuring of the active phase [2].

Catalysts Al 5 and Al 20 showed an interesting but contradictory catalytic behavior. On one hand, catalyst Al 5 has the least Al^{3+} g^{-1} clay ratio (Si/Al = 2.29) and catalyst Al 20 the highest Al^{3+} g^{-1} clay ratio (Si/Al = 1.94). Al 5 catalyst was the least affected by the incorporation of the precursor salt ($RuCl_3 \cdot 3H_2O$), since the decrease in

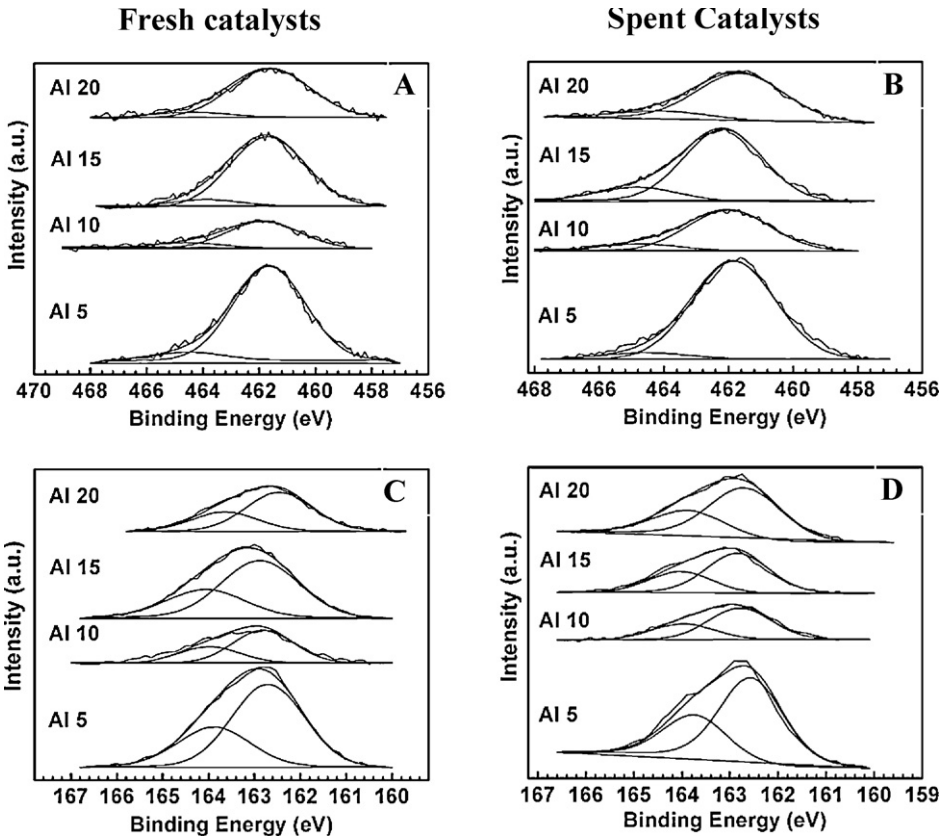

Fig. 6. Ru $3p_{3/2}$ core level spectra of: (A) sulfided catalysts and (B) spent catalysts after stability test. S 2p core level spectra of: (C) sulfided catalysts and (D) spent catalysts after stability test.

the surface area with regards to its pristine support was the lowest. According to XRD, TEM micrographs, this catalyst also maintains its morphology during the test. While XPS reveals that not great sulfur lost occurs during the test, pointing to the stability of the active phase. On the other hand, Al 20 catalyst, possessing the highest amount of aluminum incorporated, exhibits the lowest conversion although a more stable behavior than Al 10 and Al 15. The decrease in the surface area is hardly the same than Al 10 and Al 15 ones, TEM micrographs indicate that the RuS_2 phase is less dispersed but less affected by the catalytic test, while XRD and XPS point to a higher stability of the RuS_2 pyrite structure due to a lower sulfur loss during the run with regards to Al 10 and Al 15. These results suggest that the amount of aluminum incorporated is clue to stabilize the RuS_2 phase, being the catalysts presenting the lowest and the highest aluminum content the most stable catalysts.

In order to highlight the importance of the results presented here, where a natural material such as a pillared montmorillonite worked out to be a good support in hydrotreating reactions, the activity of these catalysts can be compared with that presented RuS_2 supported on a commercial γ-Al_2O_3. Thus, in a previous work [19], it has been prepared a ruthenium sulfided catalyst supported on a commercial support such as γ-Al_2O_3 and tested under the same conditions exposed here. The catalyst presented a k_{HDS} at 340 °C of 1.48 mol g_{cat}^{-1} min^{-1}, where the catalyst was more active, and much lower than the values attained here with all the catalysts at this temperature (Table 1).

4. Conclusions

Ruthenium sulfide based catalysts supported on aluminum-pillared clays were active in the HDS reaction of DBT. During catalytic testing, the catalytic activity for Al 10 and Al 15 was observed to decrease. This is probably, due to the reduction of the active phase and a change in its morphology as a consequence of the severe reaction conditions used in this catalytic process. Catalyst Al 20 presented the lowest catalytic activity, possibly attributed to a fairly dispersed active phase. However, the Al 5 sample showed a good catalytic performance due to a well dispersed active phase that inferred the highest catalytic stability throughout the test.

Acknowledgements

We gratefully acknowledge the support from the Ministry of Science and Innovation, Spain (MICINN, España) through the project MAT2009-10481, the regional government (JA) through the Excellence projects (P06-FQM-0166 and P07-FQM-5070) and FEDER funds. A.R.P. thanks the CONACyT (México) for its financial support (Scholarship No. 189933). A.I.M. also thanks the MICINN, Spain, for a Juan de la Cierva contract.

References

[1] C.S. Hsu, P.R. Robinson, Environmental Pollution Control, Practical Advances in Petroleum Processing, Springer, New York, 2006, pp. 395–447.
[2] R.R. Chianelli, G. Berhault, B. Torres, Catal. Today 147 (2009) 275–286.
[3] M. Breysse, P. Afanasiev, C. Geantet, M. Vrinat, Catal. Today 86 (2001) 5–16.
[4] M. Egorova, R. Prins, J. Catal. 224 (2004) 278–287.
[5] C. Song, X. Ma, Appl. Catal. B 41 (2003) 207–238.
[6] Z. Vít, J. Cinibulk, D. Gulková, Appl. Catal. A 272 (2004) 99–107.
[7] R.P. Toulhoat, S. Kasztelan, G. Kresse, J. Hafner, Catal. Today 50 (1999) 629–636.
[8] T.A. Pecoraro, R.R. Chianelli, J. Catal. 67 (1981) 430–445.
[9] Y. Aray, A.B. Vidal, J. Rodriguez, M.E. Grillo, D. Vega, D.S. Coll, J. Phys. Chem. C 113 (2009) 19545–19557.
[10] P. Raje, S.-J. Liaw, B.H. Davis, Appl. Catal. A 150 (1997) 319–342.
[11] P. Raje, S.-J. Liaw, B.H. Davis, Appl. Catal. A 150 (1997) 297–318.

[12] J.A. De Los Reyes, S. Göbölös, M. Vrinat, M. Breysse, Catal. Lett. 5 (1990) 17–24.
[13] J.A. De Los Reyes, M. Vrinat, C. Geantet, M. Breysse, Catal. Today 10 (1991) 645–664.
[14] M. Wojciechowska, M. Pietrowski, B. Czajka, Catal. Today 65 (2001) 349–353.
[15] F. Fréchard, P. Sautet, Surf. Sci. 336 (1995) 149–165.
[16] T. Cai, Z. Song, J.A. Rodriguez, J. Hrbek, J. Am. Chem. Soc. 126 (2004) 8886–8887.
[17] J. Quartararo, S. Mignard, S. Kasztelan, J. Catal. 192 (2000) 307–315.
[18] A. Romero-Pérez, A. Infantes-Molina, E. Rodríguez-Castellón, A. Jiménez-López, Appl. Catal. B 97 (2010) 257–268.
[19] D. Eliche-Quesada, E. Rodríguez-Castellón, A. Jiménez-López, Microporous Mesoporous Mater. 99 (2007) 268–278.
[20] K. Sapag, S. Mendioroz, Colloids Surf. A 187–188 (2001) 141–149.
[21] A. Gil, L.M. Gandía, Catal. Rev. Sci. Eng. 42 (2000) 145–212.
[22] J.M. Adams, R.W. Mccabe, in: B.K.G. Bergaya, G. Theng, Lagaly (Eds.), Handbook of Clays Science, vol. 1, Elsevier, Amsterdam, 2006, pp. 541–581.
[23] R.Q. Long, R.T. Yang, Appl. Catal. B 24 (2000) 13–21.
[24] H.J. Chae, I.S. Nam, S.B. Hong, Stud. Surf. Sci. Catal. 146 (2003) 697–700.
[25] J. Arfaoui, L.K. Boudali, A. Ghorbel, G. Delahay, Catal. Today 142 (2009) 234–238.
[26] P. Salerno, S. Mendioroz, A. López-Agudo, Appl. Catal. A 259 (2004) 17–28.
[27] M. Lenarda, L. Storaro, R. Ganzerla, R. Bertoncello, J. Mol. Catal. Mol. A: Chem. 144 (1999) 151–158.
[28] M.J. Pérez-Zurita, G. Pérez Quintana, G.J. Biomorgi, C.E. Scott, Prepr. Symp. Am. Chem. Soc. Div. Fuel Chem. 48 (1) (2003) 90–91.
[29] O. Exner, Nature 227 (1970) 366–367.
[30] R.A. Pis-Diez, H. Jubert, J. Mol. Catal. 83 (1993) 219–235.
[31] G. Berhault, M. Lacroix, M. Breysse, F. Maugé, J.C. Lavalley, H. Nie, L. Qu, J. Catal. 178 (1998) 555–565.
[32] M. Breysse, G. Berhault, S. Kasztelan, M. Lacroix, F. Maugé, G. Perot, Catal. Today 66 (2001) 15–22.
[33] K.G. Knudsen, B.H. Cooper, H. Topsøe, Appl. Catal. A 189 (1999) 205–215.
[34] J. Rouquerol, F. Rouquerol, K. Sing, Adsorption by Powders and Porous Solids Principles, Methodology and Applications, Academic Press, London, 1999, pp. 355–399 (Chapter 11).
[35] G. Leofanti, M. Podovan, G. Tozzola, B. Venturelli, Catal. Today 41 (1998) 207–219.
[36] J.F. Moulder, W.F. Stickle, P.E. Sobol, K.D. Bomben, in: J. Chastain (Ed.), Handbook of X-ray Photoelectron Spectroscopy, Perkin-Elmer, Minnesota, 1992, pp. 114–115.
[37] V. Mazzieri, F. Coloma-Pascual, A. Arcoya, P.C. L'Argentière, N.S. Fígoli, Appl. Surf. Sci. 210 (2003) 222–230.
[38] F.A. Cotton, G. Wilkinson, C.A. Murillo, M. Bochman, Advanced Inorganic Chemistry, John Wiley and Sons Inc., USA, 1999, pp. 1012–1013.
[39] S.E. Livingstone, in: J.C. Bailar, M.J. Emeléus, R. Nyholm, A.F. Trotman-Dickenson (Eds.), Comprehensive Inorganic Chemistry, vol. 3, Pergamon Press, Oxford, 1973, pp. 1191–1193.
[40] P.C.H. Mitchell, C.E. Scott, J.P. Bonnelle, J.G. Grimblot, J. Catal. 107 (1987) 482–487.